47th AIAA Aerospace Sciences Meeting Including The New Horizons Forum and Aerospace Exposition
5 - 8 January 2009, Orlando, Florida
AIAA 2009-148

47th AIAA Aerospace Sciences Meeting and Exhibit, January, 2009, Orlando, Florida

Design of Adjoint Based Laws for wing flutter control

Karthik Palaniappan*, Pradipta Sahu†, Juan Jose Alonso‡
and Antony Jameson§

I. Introduction

An airplane, by its nature of being, is constructed so that it is as light as possible. The structural design is guided by static and dynamic factors. The more stringent constraints on the structural design are due to dynamic loads, caused by aero-elastic interactions. One of the most commonly encountered problems in aeroelasticity is flutter,[1] a term that is used to recognize the transfer of energy from unsteady aerodynamics associated with the surrounding fluid to the wing structure, resulting in rapidly divergent behaviour. If flutter can be controlled at cruise speeds, we can design lighter wings and consequently more efficient airplanes. It is therefore, in the aircraft designer's best interest to design innovative ways in which flutter can be controlled without making the resulting structure too heavy.

There are three important choices to make while designing active control strategies for suppressing flutter. The first is the choice of actuator. In this paper, the actuators we use are jets in the walls through which there is a small mass flow, either by way of blowing or suction. The second is to define a clear control objective. Finally, we need to design a control law that will make suitable state measurements and drive the actuators so that the desired control objective is achieved.

The concept of Active Flow Control is fast gaining popularity in Fluid Mechanics circles. Indeed, it is important to realize that adding or removing fluid at the wing surface is equivalent to effecting a shape modification. Flow control using surface jets should, in principle, have an effect very similar to that of morphing surfaces.

The capability to directly alter the flow field offers a huge realm of possibilities. Seifert, Theofilis and Joslin[2] categorize the problems that are amenable to using Active Flow Control:

1. Separation (Delay, Reattachment, Stabilization, etc.)
2. Transition (Delay, Promotion)
3. Jet (Spreading, Vectoring, Acoustics)
4. Drag Reduction (Laminar Skin Friction, Turbulent separation control)
5. Thermal Management (Cooling, heating, reduced signature)
6. Guidance, Propulsion and Control (Mild hinge-less maneuvering, gust alleviation)
7. Vortex Dominated Flows
8. Combustion, Turbo machines (Inlets, rotors, stators and diffusors)
9. Cavity (noise, vibration)
10. Optical Distortion

*Aerospace Engineer, Austin, Texas
†Cessna Corporation, Wichita, Kansas
‡Associate Professor, Stanford University
§Professor, Stanford University

While different types of actuators can be designed for active flow control, Zero Net Mass Flux (ZNMF) Synthetic Jets are gaining popularity as the actuator of choice. A ZNMF synthetic jet is popular for the main reason that it is formed entirely from the working medium of the flow. These eject and remove mass from the flow system through a narrow orifice periodically. This results in altering the momentum field around the orifice without adding or removing mass from the flow. The primary considerations in the design of synthetic jets are the size and positioning of the orifice, and the time frequency of actuation. The design of synthetic jets and the physics of their interaction with a cross-flow are discussed in detail by Glezer and Amitay.[3]

Flow control, for aerodynamics, using synthetic jets has been studied experimentally by Amitay,[4] Tuck and Soria,[5] and Nishizawa et al.[6,7] Numerical investigations were performed by Nae.[8] It should be noted that in all these experiments, the location and frequencies of the actuators were chosen apriori. The control implemented, therefore, is open loop.

The study of closed loop active flow control techniques is still in its primitive stages. This is because designing a closed loop (*feedback*) control law requires understanding of the system dynamics. In spite of the fact that it is possible to obtain numerical solutions to the *Navier-Stokes* equations, understanding of the behavior of a flow-actuator system is extremely limited.

Feedback laws based on Reduced Order Models have been derived by Samimy *et al.*,[9] Kumar and Tewari[10] and Cohen *et al.*[11] The major drawback of these efforts is that the actuator dynamics are not modeled as part of the reduced order description of the system.

All previous attempts at flow control have either involved designing simplistic controls for complex problems or complex *feedback* based controls for simple problems. Problems like separation control, drag reduction and control of the vortex shedding frequency in the flow past a cylinder have all been controlled using open loop controllers.

Closed loop control has been demonstrated only on simplistic models derived from simulation or experiment.

An *Ideal Flow Control Law* should have the following properties:

1. Broadly applicable: we are looking for an algorithmic framework for generating flow control laws for a variety of problems. The development of such a framework would enable easy analysis and design of control laws for a variety of flow control problems.

2. Scientific: the control laws should be based on a realistic model of the fluid system.

3. Robust: should account for variability in measurement, actuation, etc. This would mean that the control u should be *feedback* based
$$u = F(x), \tag{I.1}$$
where x is the current system state.

Our goal, therefore, is to develop *feedback* based control laws that are derived from a realistic representation of the flow. We try to make sure that the framework is as generic as possible, lending easy extension to a variety of situations. We then discuss specific applications of the control law thus derived, including control of Flutter.

The concept of flow control, as described in this paper, relies heavily on the Adjoint Methods derived by Jameson and his associates over the last few years[12] and.[13] The control law that is derived is based on a 2-d model. This is then scaled up to 3 dimensions and 3-d simulations are performed to see if flutter can be controlled using this new law.

II. Flutter Simulation

A. Flow Model: The Euler Equations for Fluid Flow with Blowing at the Walls

In this paper, the fluid flow is modeled using the Euler Equations. The Euler Equations model the behaviour of invicid, compressible fluids. They are
$$\frac{\partial \mathbf{w}}{\partial t} + \frac{\partial \mathbf{f_i}}{\partial x_i} = 0 \, . \tag{II.1}$$

Here x_i represent the cartesian co-ordinate directions, $\mathbf{w}$ the state variables, and $\mathbf{f_i}$ are the corresponding flux vectors, given by

$$\mathbf{w} = (\rho, \rho\mathbf{u}, \rho\mathbf{v}, \rho\mathbf{w}, \rho\mathbf{E}) \ , \tag{II.2}$$

and,

$$\mathbf{f_i} = (\rho\mathbf{u_i}, \rho\mathbf{u_i}\mathbf{u} + \delta_{\mathbf{i1}}\mathbf{P}, \rho\mathbf{u_i}\mathbf{v} + \delta_{\mathbf{i2}}\mathbf{P}, \rho\mathbf{u_i}\mathbf{w} + \delta_{\mathbf{i3}}\mathbf{P}, \rho\mathbf{u_i}\mathbf{H}) \ . \tag{II.3}$$

The Steady State Euler Equations can be written in weak conservation form as follows

$$\int_{\mathcal{B}} n_i \phi^T f_i(w) d\mathcal{B} = \int_{\mathcal{D}} \frac{\partial \phi^T}{\partial x_i} f_i(w) d\mathcal{D} \ , \tag{II.4}$$

where ϕ is any test function. If a transformation is made from physical space to computational space, defined by the mapping functions

$$K_{ij} = \left[\frac{\partial x_i}{\partial \varepsilon_j}\right] \ , \quad J = det(K) \ , \quad K^{-1}_{ij} = \left[\frac{\partial \varepsilon_i}{\partial x_j}\right] \ , \tag{II.5}$$

and

$$S = JK^{-1} \ , \tag{II.6}$$

the Euler Equations (II.4) become

$$\int_{\mathcal{B}_\xi} n_i \phi^T S_{ij} f_j(w) d\mathcal{B}_\xi = \int_{\mathcal{D}_\xi} \frac{\partial \phi^T}{\partial \xi_i} S_{ij} f_j(w) d\mathcal{D}_\xi \ . \tag{II.7}$$

The boundary conditions for the case where we have blowing or suction at the boundary can then be prescribed in terms of the blowing velocity as follows

$$F_2 = (\rho q_n, \rho q_n u + S_{21}P, \rho q_n v + S_{22}P, \rho q_n w + S_{23}P, \rho q_n H) \ , \tag{II.8}$$

where ρq_n is the prescribed mass flow at the boundary, initially set to zero in the design problem.

B. Structural Model

The structural dynamic model is derived from the theory of elasticity, which relates the deformation and internal stresses of the structure to the external loads applied. A Lagrangian frame is used to describe the structure, as contiguous elements of the structure continue to remain contiguous unless structural failure occurs.

The state of structure at any point in time, is represented at each spatial point by 15 state variables. There are three displacements $\mathbf{u}$, which represent the deviation of the point from its baseline position. Additionally, the internal state of the structure is represented by the stress and strain tensors, σ_{ij} and ϵ_{ij} respectively, both of which are symmetric and hence have six independent components each.

The normal stress is defined as the force acting in a given direction, per unit area normal to that direction. Shear stress is defined as the force acting tangential to a surface, per unit area. Strains are the ratio of the displacement of a point in a particular direction to the original dimension of the object at that point.

There are six equations which relate the strains to the displacements. These are linear for the case of small deformations.

$$\epsilon_{ii} = \frac{\partial u_i}{\partial x_i}, \quad \epsilon_{ij} = \epsilon_{ji} = \frac{\partial u_i}{\partial x_j} + \frac{\partial u_j}{\partial x_i} \ . \tag{II.9}$$

The stresses are related to the strains by six constitutive relationships. If the material is isotropic, these reduce to

$$\sigma_{ii} = \frac{E}{(1+\nu)(1-2\nu)} \left[(1-\nu)\epsilon_{ii} + \nu(\epsilon_{jj} + \epsilon_{kk})\right], \quad \sigma_{ij} = \sigma_{ji} = \frac{E}{2(1+\nu)}\epsilon_{ij} \ , \tag{II.10}$$

where E is the Young's modulus of the material, and ν is the Poisson's ratio. The external forces can be related to the internal stresses and strains using the Newton's laws.

$$\frac{\partial \sigma_{ij}}{\partial x_j} + \rho \frac{\partial^2 u_i}{\partial t^2} + \kappa \frac{\partial u}{\partial t} = F_i \ . \tag{II.11}$$

Here ρ is the density of the material, κ is the damping factor, and $\mathbf{F}$ is the applied external force. Solving these fifteen equations gives us the stress – strain – displacement distribution throughout the structure.

In the present paper we will first investigate the aeroelastic behavior and control of a 2-d airfoil whose schematics is shown in Figure II.1. We will then use the information derived from the 2-d study, and derive the control laws for a 3-d wing.

A 2-d airfoil model can be shown to be a fair representation for flutter prediction as shown by Theodorson and Garrik[14] of a straight wing of a large span by giving it the geometric and inertial properties of the cross-section three quarters of the way from the centerline to the wing tip. The equations of motion of this simple system can be shown to be as follows.

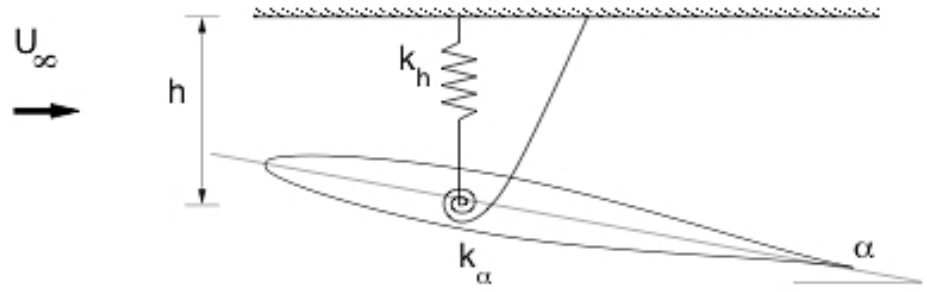

Figure II.1. Typical Section Wing Model Geometry

$$m\ddot{h} + S_\alpha \ddot{\alpha} + K_h h = -L \tag{II.12}$$

$$S_\alpha \ddot{h} + I_\alpha \ddot{\alpha} + K_\alpha \alpha = M_{ea} \tag{II.13}$$

K_h and K_α are representative of the bending and torsional stiffness of the wing about its elastic axis. The elastic axis is the locus of points about which, if a force is applied, doesn't result in any rotation about that point. m and I_α are the mass and moment of inertia of the wing section about the elastic axis. S_α is the coupling term which depends on the relative position of the center of gravity and the elastic axis.

For the present paper we assume the structural properties to be fixed and we have some amount of control of the right hand sides of the equations via blowing and suction. The objective is to find a suitable control law which will modify the aerodynamic terms so as to prevent flutter.

C. Computational Simulation

The flow is simulated by solving the unsteady *Euler* equations. The *Euler* equations are solved using a dual time stepping method, using a third order backward difference formula in time, and a symmetric Gauss Seidel scheme for solving the inner iterations. The above mentioned flow simulation code is integrated with a two degree of freedom structural model given for the 2-d simulation. For the 3-d simulation, the complete 3-d elastic equations derived in the previous section are solved using a nonlinear Finite Element solver, FEAP.[15]

The aerodynamic and structural solvers are coupled by exchanging information at regular intervals during the convergence process. A diagram representing the aeroelastic iteration is shown in Figure II.2. At the start of each iteration the surface pressures are translated into nodal forces and the structural solver is called. The new displacement field is then translated to a movement of the CFD mesh and then flow iterations are performed. While making the transfer of one must make sure that the transfer of load is consistent and conservative.[16] By consistency we mean that the sum of the structural forces must be the same as that of the CFD loads.

$$\sum \underline{\mathrm{f}}_S = \int \underline{\mathrm{P}}.d\underline{\mathrm{A}}, \tag{II.14}$$

Conservation stipulates that the virtual work performed by the load vector, $\underline{\mathrm{f}}_S$, undergoing a virtual displacement of the structural model, $\delta\underline{\mathrm{u}}_S$, must be equal to the work performed by the CFD forces, undergoing the equivalent displacement of the CFD surface mesh, $\delta\underline{\mathrm{x}}$.

$$\delta W_{\mathrm{S}} = \underline{\mathrm{f}}_S \delta\underline{\mathrm{u}}, \tag{II.15}$$

while the virtual work performed by the fluid acting on the surface of the CFD surface mesh is given by

$$\delta W_{\mathrm{A}} = \underline{\mathrm{f}}_A \delta \underline{\mathrm{x}} \tag{II.16}$$

For a conservative scheme, $\delta W_{\mathrm{A}} = \delta W_{\mathrm{S}}$

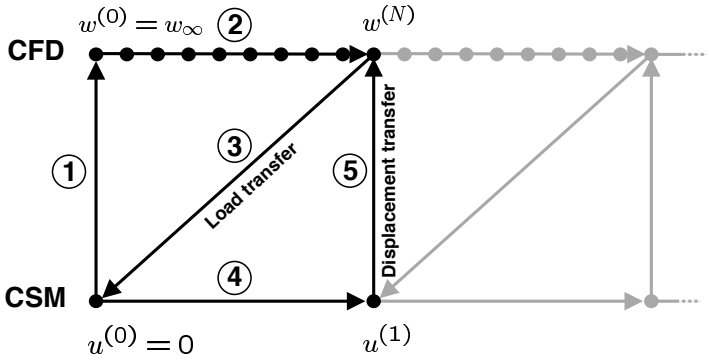

Figure II.2. The aero-structural iteration procedure.

The coupled aero-structural system is integrated using the *Newmark* scheme. The simulation techniques are discussed in detail in the first author's Ph. D. thesis.[17]

III. Derivation of Adjoint Based Control Laws

A. System Linearization and Model Order Reduction

In Equations (II.12) and (II.13), the structural parameters are constant. The lift L and the moment M are complex nonlinear functions of the system state $\mathbf{w}$, α, $\dot{\alpha}$, h and $\dot{h}$. Moreover, α, $\dot{\alpha}$, h and $\dot{h}$ are itself functions of the system state $\mathbf{w}$. Here the state $\mathbf{w}$ is the vector consisting of all the *Euler* states at all finite volumes used in the simulation. Thus

$$L = L(\mathbf{w}, \mathbf{u}) , \tag{III.1}$$

$$M = M(\mathbf{w}, \mathbf{u}) . \tag{III.2}$$

Linearizing about the nominal operating point, we get

$$L = \frac{\partial L}{\partial \mathbf{w}}^T \delta\mathbf{w} + \frac{\partial L}{\partial \mathbf{u}}^T \delta\mathbf{u}, \tag{III.3}$$

$$M = \frac{\partial M}{\partial \mathbf{w}}^T \delta\mathbf{w} + \frac{\partial M}{\partial \mathbf{u}}^T \delta\mathbf{u}. \tag{III.4}$$

It should be noted that for a simulation with one million finite volumes, the dimension of $\mathbf{w}$ is four million for a 2-d simulation and five million for a 3-d simulation. Thus evaluating the above derivatives is a formidable computational challenge. It is also important to recognize that not all the derivatives are significant in the above representation. Consider, for example, a cell in the far-field. The value of the state variables there is not going to change by much, however rapid the oscillations. Therefore, it is of very little use evaluating these derivatives in our linearized model.

Instead, we choose to obtain a suitable reduced order model that captures the essential physics. The most obvious reduction that we can obtain is in terms of α, $\dot{\alpha}$, h and $\dot{h}$. We therefore work with a model of the form:

$$L = L_\alpha \alpha + L_{\dot{\alpha}} \dot{\alpha} + L_h h + L_{\dot{h}} \dot{h} + \frac{\partial L}{\partial \mathbf{u}}^T \mathbf{u}, \tag{III.5}$$

$$M = M_\alpha \alpha + M_{\dot{\alpha}} \dot{\alpha} + M_h h + M_{\dot{h}} \dot{h} + \frac{\partial M}{\partial \mathbf{u}}^T \mathbf{u}. \tag{III.6}$$

Equations (III.5) and (III.6) assume that the nominal values of α, $\dot{\alpha}$, h and $\dot{h}$ and $\mathbf{u}$ are zero, respectively. Thus for the flutter control problem being studied, the following state vector is used:

$$\mathbf{x} = [\alpha \quad \dot{\alpha} \quad h \quad \dot{h}]^T \tag{III.7}$$

B. System Identification: Evaluation of Sensitivities

In our aero-strucutral model, the lift L and the moment M depend on the complete system state $\mathbf{w}$. However, using a full order state model to design a controller is not feasible, given the extremely high dimensionality of the system. We therefore, formulate a reduced order model of the system. In order for this model to be complete, we need to evaluate the sensitivities with respect to the reduced order state $\mathbf{x}$ and the control variables $\mathbf{u}$.

1. Sensitivities with respect to the state variables

The sensitivities of the lift and moment with respect to the state variables are evaluated in two different ways.

THEODORSEN THEORY: First, we use theoretical results from Theodorsen.[1] Theodorsen theory assumes that the airfoil under consideration is thin, and is oscillating in an incompressible flow. Under these considerations

$$\begin{aligned} L_\alpha = \pi\rho v_\infty^2 c \quad &, \quad L_{\dot{\alpha}} = \frac{\pi\rho v_\infty c^2}{4}, \\ L_h = 0 \quad &, \quad L_{\dot{h}} = \pi\rho v_\infty c, \\ M_\alpha = \frac{\pi\rho v_\infty^2 c^2}{4} \quad &, \quad M_{\dot{\alpha}} = 0, \\ M_h = 0 \quad &, \quad M_{\dot{h}} = \frac{\pi\rho v_\infty c^2}{4}, \end{aligned}$$

Here ρ is the freestream density, v_∞ is the freestream velocity and c is the chord of the airfoil.

LEAST-SQUARES METHOD: In the second method, we evaluate the sensitivities, by studying the unforced response of a pitching airfoil, and then estimating the sensitivities by a least-squares technique. The aero-structural response of the system over a period of time is similar to the unforced response reproduced in Figures IV.3, IV.4, IV.5 and IV.6. These simulations provide numerical values for

$$\begin{aligned} \alpha &= f_1(t) \\ \dot{\alpha} &= f_1'(t) \\ h &= f_2(t) \\ \dot{h} &= f_2'(t) \\ L &= f_3(t) \\ M &= f_4(t) \end{aligned}$$

We now try to fit the data thus obtained to functions of the form

$$\begin{aligned} L &= L_\alpha\alpha + L_{\dot{\alpha}}\dot{\alpha} + L_h h + L_{\dot{h}}\dot{h}, \\ M &= M_\alpha\alpha + M_{\dot{\alpha}}\dot{\alpha} + M_h h + M_{\dot{h}}\dot{h}. \end{aligned}$$

Our goal is to evaluate the sensitivities L_α, $L_{\dot{\alpha}}$, L_h, $L_{\dot{h}}$, M_α, $M_{\dot{\alpha}}$, M_h and $M_{\dot{h}}$. We do this using a least-squares technique.

It can be seen from the simulation results that both techniques work quite well. The system identification by the least-squares technique, works slightly better, in the sense, it achieves faster stabilization. This can be attributed to the fact that this represents the nonlinear system more closely.

2. Sensitivities with respect to the control variables

We also need to evaluate the sensitivities of L and M with respect to the control variables $\mathbf{u}$, $\frac{\partial L}{\partial \mathbf{u}}$ and $\frac{\partial M}{\partial \mathbf{u}}$ respectively. We do this are using an *Adjoint* method. In our case, the control variable is the normal mass flux at the wall ρq_n.

Let us assume that we are trying to find the sensitivities due to the control variables of a function I given by:

$$I = \int_{\mathcal{B}_\xi} \mathcal{M}(w, \rho q_n) d\mathcal{B}_\xi \ , \tag{III.8}$$

The constraint is given by the Euler Equations (II.7,II.8). Since equation II.7 is true for any test function ϕ, we can choose ϕ to be the adjoint variable ψ. We can then add the constraint given by the Euler Equations to III.8 to form the augmented cost function given by

$$\begin{aligned} I &= \int_{\mathcal{B}_\xi} \mathcal{M}(w, \rho q_n) d\mathcal{B}_\xi \\ &- \int_{\mathcal{B}_\xi} n_i \psi^T S_{ij} f_j(w, \rho q_n) d\mathcal{B}_\xi \\ &+ \int_{\mathcal{D}_\xi} \frac{\partial \psi^T}{\partial \xi_i} S_{ij} f_j(w, \rho q_n) d\mathcal{D}_\xi \ . \end{aligned} \tag{III.9}$$

Taking the first variation of the Function I we have

$$\begin{aligned} \delta I &= \int_{\mathcal{B}_\xi} \left(\frac{\partial \mathcal{M}}{\partial w} \delta w + \frac{\partial \mathcal{M}}{\partial \rho q_n} \delta(\rho q_n) \right) d\mathcal{B}_\xi \\ &- \int_{\mathcal{B}_\xi} n_i \psi^T S_{ij} \left(\frac{\partial f_j}{\partial w} \delta w + \frac{\partial f_j}{\partial \rho q_n} \delta(\rho q_n) \right) d\mathcal{B}_\xi \\ &+ \int_{\mathcal{D}_\xi} \frac{\partial \psi^T}{\partial \xi_i} S_{ij} \left(\frac{\partial f_j}{\partial w} \delta w + \frac{\partial f_j}{\partial \rho q_n} \delta(\rho q_n) \right) d\mathcal{D}_\xi \ . \end{aligned} \tag{III.10}$$

We can then choose our co-state variables ψ so that it satisfies the adjoint equations

$$S_{ij} \frac{\partial f_j}{\partial w}^T \frac{\partial \psi}{\partial w} = 0 \ , \text{on } \mathcal{D}_\xi \ , \tag{III.11}$$

and

$$\frac{\partial \mathcal{M}}{\partial w} = \psi^T \frac{\partial F_2}{\partial w} \ , \text{on } \mathcal{B}_\xi \ . \tag{III.12}$$

We also observe that

$$\frac{\partial f_j}{\partial \rho q_n} = 0 \ , \text{on } \mathcal{D}_\xi \ . \tag{III.13}$$

The expression for the adjoint gradient then becomes

$$\begin{aligned} \delta I &= \int_{\mathcal{B}_\xi} \left(\frac{\partial \mathcal{M}}{\partial \rho q_n} \delta(\rho q_n) \right) d\mathcal{B}_\xi \\ &- \int_{\mathcal{B}_\xi} \left(\psi_1 + \psi_2 u + \psi_3 v + \psi_4 w + \psi_5 \left(E + \frac{P}{\rho} \right) \right) \delta \rho q_n d\mathcal{B}_\xi \ . \end{aligned} \tag{III.14}$$

The gradient is then modified to account for the fact that the nett. mass flow through the boundaries is zero. This gives the matrix B from (**??**).

C. Flutter Control: Formulation of the Objective Function

We can define the flutter velocity as that point where we have sustained oscillations of the system. Let us define the state vector $\mathbf{x}$ as follows

$$\mathbf{x} = [\alpha \quad \dot{\alpha} \quad \mathbf{h} \quad \dot{\mathbf{h}}]^{\mathbf{T}} \tag{III.15}$$

The control vector $\mathbf{u}$ is the vector of blowing/suction velocities at the wall. The dynamics of the system is represented by the equations derived in Section II. For the purposes of designing a controller, we model the lift L and the moment M using a reduced order model as presented in Equations (III.5) and (III.6). The system model used to design a controller is then

$$\begin{aligned} m\ddot{h} + S_\alpha \ddot{\alpha} + K_h h &= -\left(L_\alpha \alpha + L_{\dot{\alpha}} \dot{\alpha} + L_h h + L_{\dot{h}} \dot{h} + \frac{\partial L}{\partial \mathbf{u}}^T \mathbf{u} \right) \\ S_\alpha \ddot{h} + I_\alpha \ddot{\alpha} + K_\alpha \alpha &= \left(M_\alpha \alpha + M_{\dot{\alpha}} \dot{\alpha} + M_h h + M_{\dot{h}} \dot{h} + \frac{\partial M}{\partial \mathbf{u}}^T \mathbf{u} \right). \end{aligned}$$

This can be re-phrased in state space form as follows:

$$M\dot{\mathbf{x}} = \hat{A}\mathbf{x} + \hat{\mathbf{B}}\mathbf{u}. \tag{III.16}$$

Here the matrix $\hat{B}$ represents the sensitivities of the state vectors with respect to the control variables. This can be obtained by solving the *Adjoint* equations. Inverting M, we get a system of the form

$$\dot{\mathbf{x}} = A\mathbf{x} + \mathbf{B}\mathbf{u}. \tag{III.17}$$

It is possible to design a controller for the system (III.17) using LQR techniques.

The objective of the problem is to control the system given by (III.17), so that the final value of the state vector is given by

$$\mathbf{x_f} = [\alpha_\mathbf{f} \quad \mathbf{0} \quad \mathbf{h_f} \quad \mathbf{0}]^\mathbf{T} \tag{III.18}$$

If this is rephrased as an optimization problem, the objective would be to minimize the following function:

$$J = \frac{1}{2} \int_0^T \left((\mathbf{x} - \mathbf{x_f})^T Q (\mathbf{x} - \mathbf{x_f}) + \mathbf{u}^T R \mathbf{u} \right) \, dt \tag{III.19}$$

where Q is a positive semi-definite weighting matrix and R is a positive definite matrix. In our case,

$$\begin{aligned} Q &= I, \\ R &= \varepsilon I, \end{aligned}$$

where I is the identity matrix, and ε is a small positive constant. R is required to be positive definite, to ensure that the control computed is not of unreasonable magnitudes.

D. Backsubstitution of the Control Law into the Nonlinear System

A *Feedback* control gain matrix can be derived for the flutter control problem by solving the Riccatti equation.[18] Now, the aero-structural system is simulated with blowing and suction control applied at the actuator locations. The magnitude of control required at each actuator location is given by the control gain matrix K_{ss}

$$\mathbf{u} = K_{ss}\mathbf{x}. \tag{III.20}$$

The results are presented in the next section. It can be seen that this control law is successful in stabilizing the system.

E. Extension of the 2-d control law to 3 dimensions

The 2-d problem provides for values of flow velocities at the boundary that serve to control the flutter of a 2-d section. The 2-d problem has been shown to be representative of a 3-d problem where the wing section chosen is that at the 3/4th span of the wing. We will experiment with ways of scaling these control velocities at the 3/4th point across the wing such that the flutter of the entire wing can be controlled. These results will be analyzed and presented.

IV. Results

A. 2-d Results

The following experiments were conducted on a symmetric NACA 0012 airfoil at a freestream Mach number of 0.3. A 160×32 grid was used for the CFD simulation.

The structural properties were chosen as follows: $I_\alpha = 60$, $M = 60$, $K_h = 60$, $K_\alpha = 60$, and $S_\alpha = 30$. Our nominal rest point is $\alpha = 0^\circ$ and $h = 0$.

1. *Adjoint Gradients*

As discussed in the last section, the *Adjoint* method is used to find the gradients of lift and moment with respect to the control variables, namely the blowing and suction velocities on the surface. It should be noted that this is done using a steady flow assumption about the nominal rest point of the system. We used a symmetric NACA 0012 section. So for our case, this nominal rest point was at $\alpha = 0$, and $h = 0$. These gradients are shown in Figures IV.1 and IV.2.

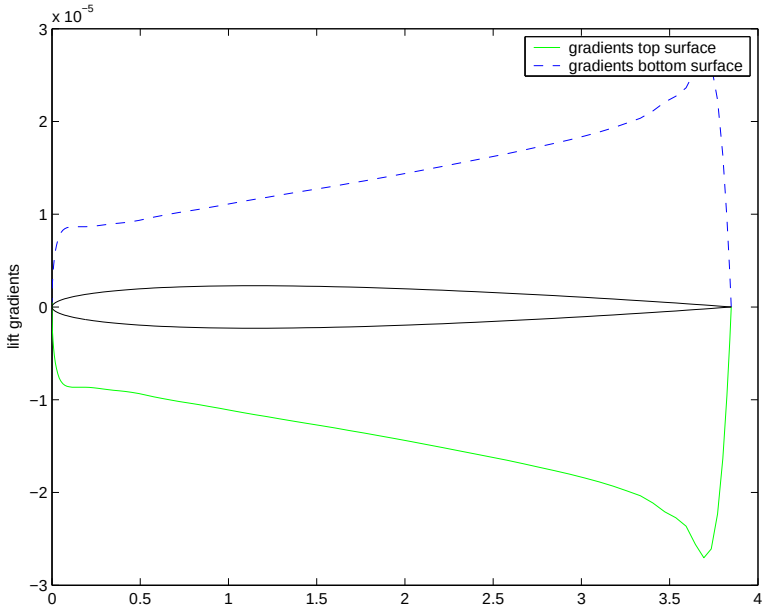

Figure IV.1. Gradient of lift with respect to control mass fluxes

2. *Application of Feedback Control to the Nonlinear Flutter Problem*

The uncontrolled and controlled aero-structural simulations are represented in Figures IV.3, IV.4, IV.5, and IV.6. It should be noted that even though the *feedback* law is derived from a linearized model of the system, the control is applied to a complete nonlinear model. Two different methods are used to find the aerodynamic derivatives. It can be seen that the least-squares method does a better job than the Theodorsen method for flutter control. This is obvious because this represents the nonlinear system more accurately. The corresponding blowing/suction velocities are shown in Figure IV.7. It should be noted that the freestream value of ρq_n in our simulation was 1. So the values of blowing and suction controls required is quite small. Moreover, we need zero control input at the equilibrium point, which is what we desire.

3. *Time step refinement studies*

To ensure that the flutter control simulations are correct, the time step for the nonlinear aero-structural solver is made smaller and smaller and the controlled behaviour is observed. It can be seen that the pattern of variation of the angle of attack with time is fairly well predicted by the solver. (See Figure IV.8).

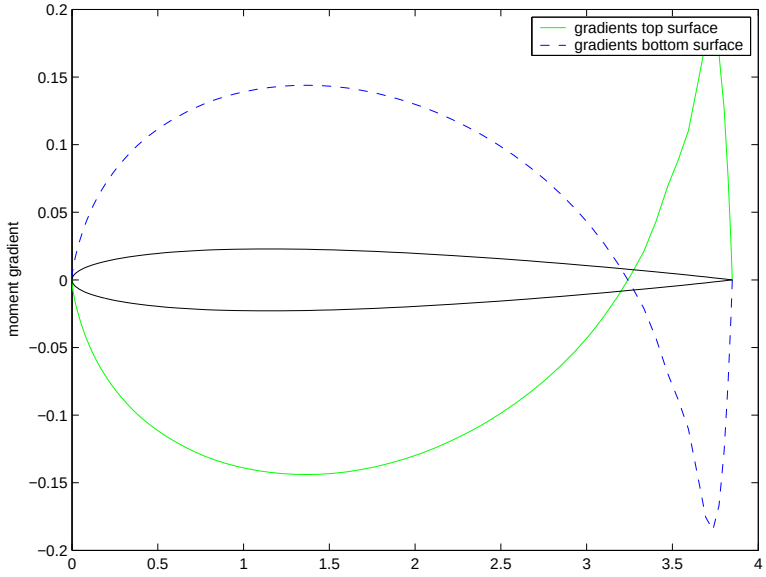

Figure IV.2. Gradient of moment with respect to control mass fluxes

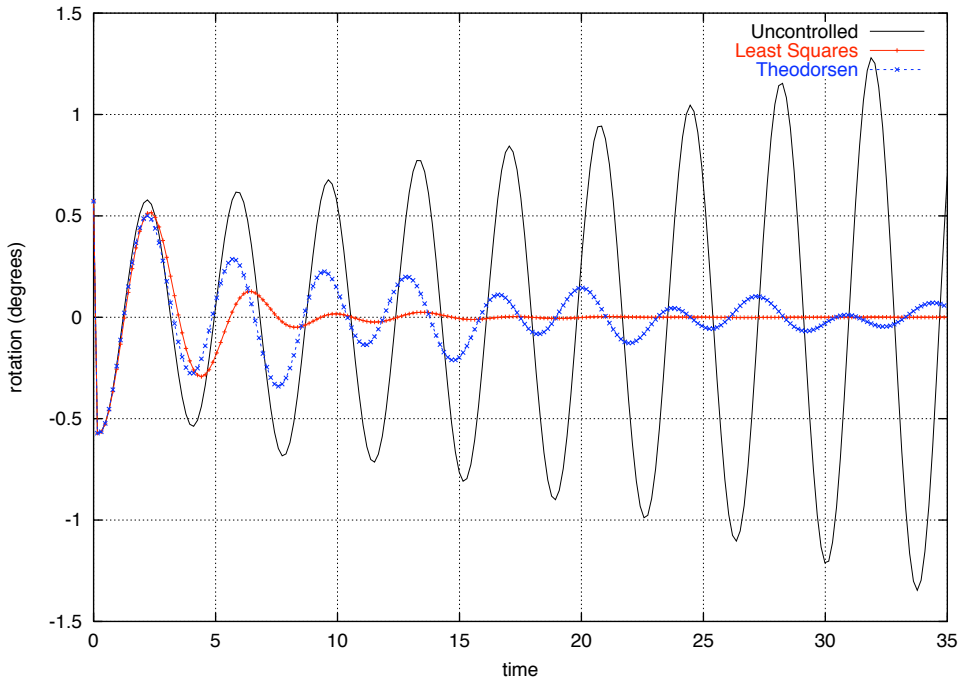

Figure IV.3. Variation of angle of attack (degrees) with time: controlled and uncontrolled cases

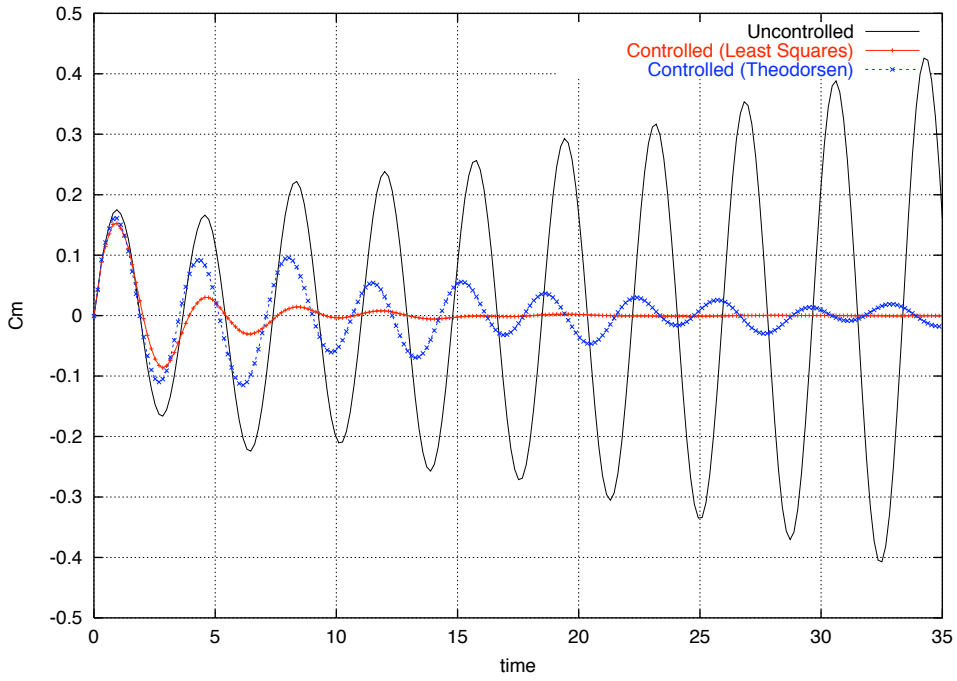

Figure IV.4. Variation of C_m with time: controlled and uncontrolled cases

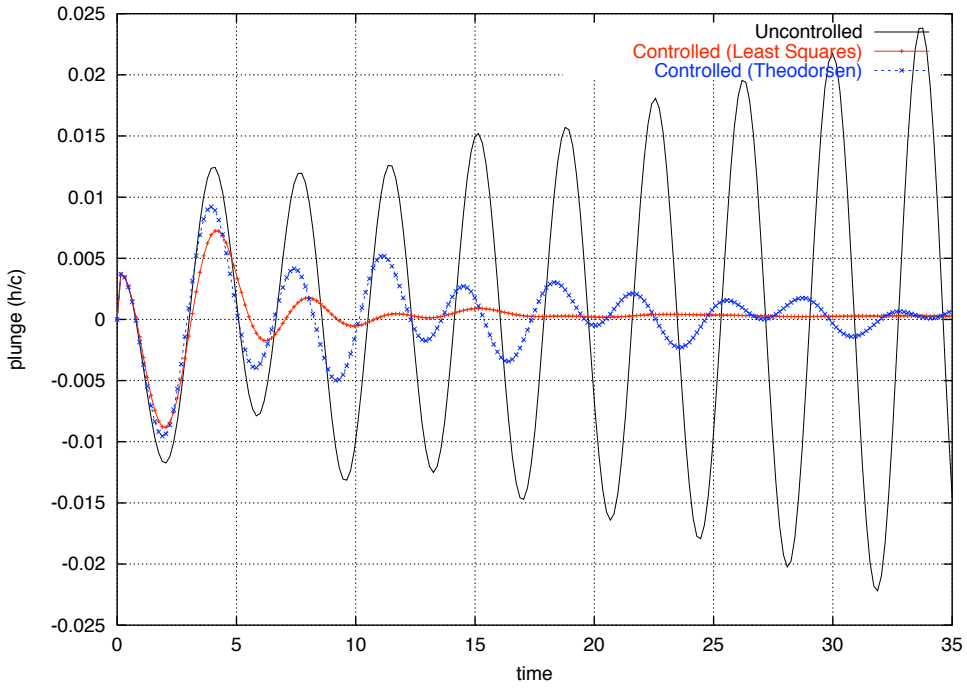

Figure IV.5. Variation of plunge h/c with time: controlled and uncontrolled cases

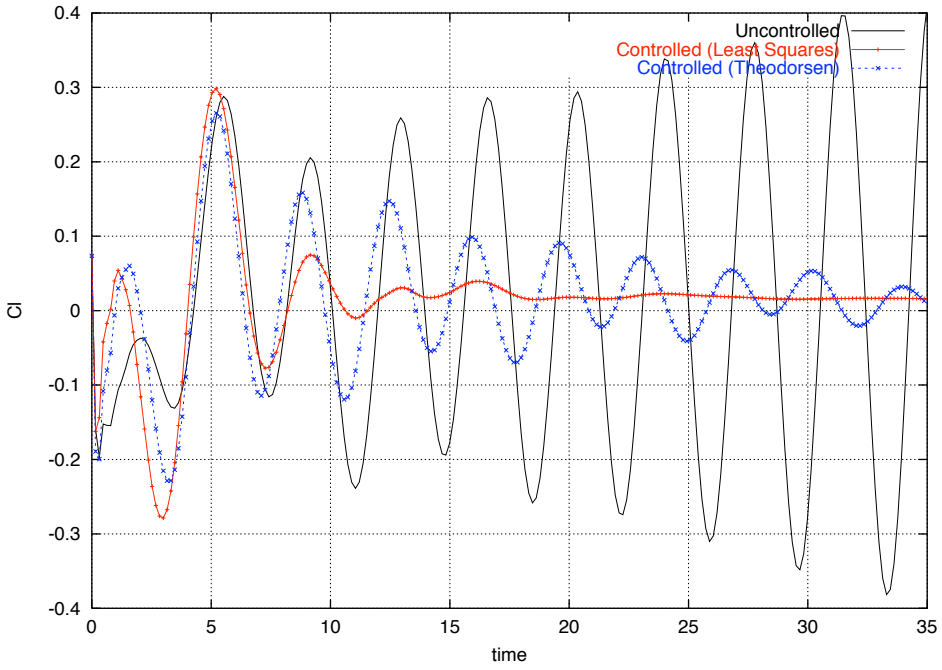

Figure IV.6. Variation of C_l with time: controlled and uncontrolled cases

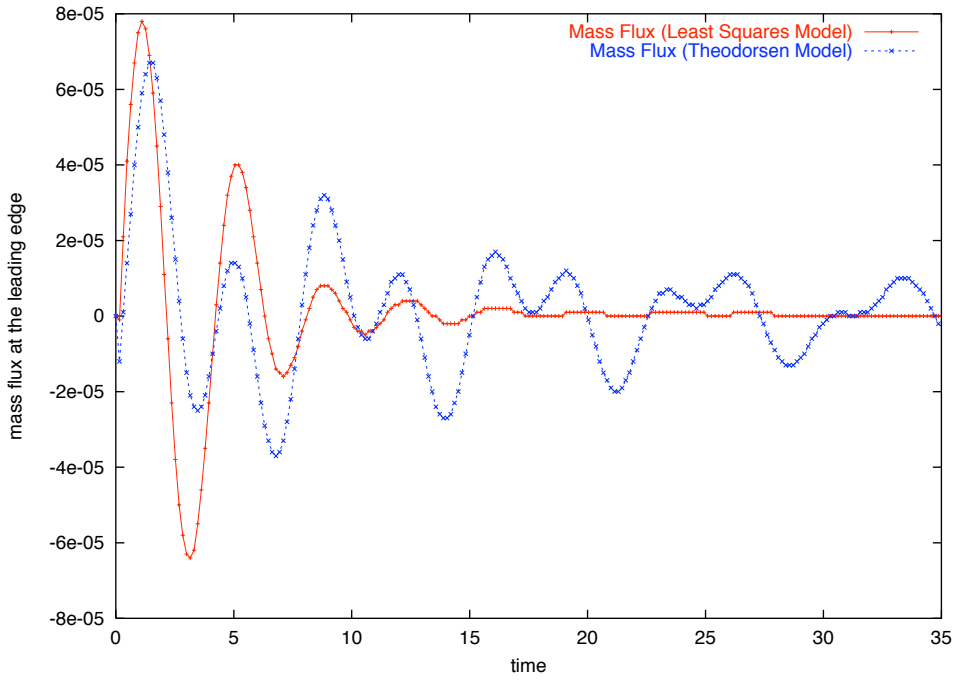

Figure IV.7. Blowing/Suction mass fluxes at the Leading Edge

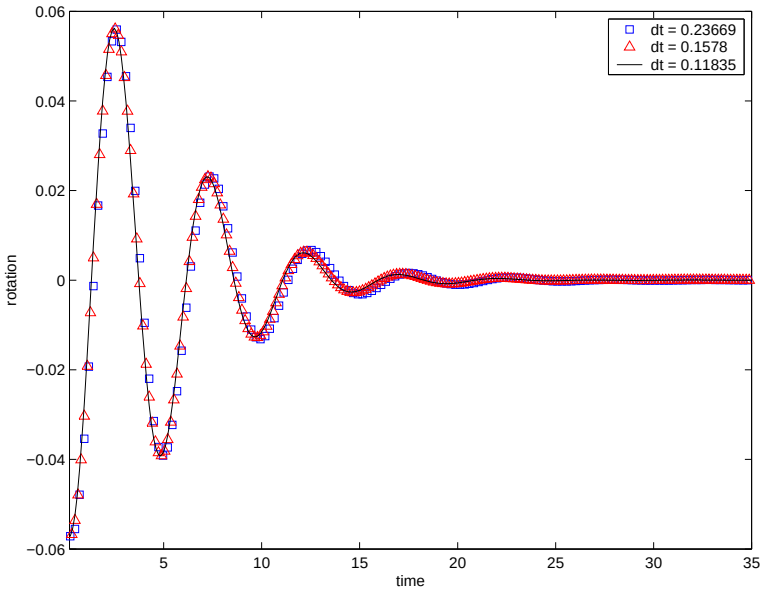

Figure IV.8. Time step refinement studies for the variation of angle of attack with time

4. Reduction in the number of Actuators

Our next step is to specialize the control law thus derived to work when the number of actuators is finite. It was found that flutter could be controlled with as few as four actuators: one each in the leading and trailing edges and one each in the middle of the upper and lower surfaces. The fact that there are only four actuation points is represented by zeroing out the gradient shown in Figures IV.1 and IV.2 everywhere except at these four locations. (Every location is represented by a small cluster of CFD cells to prevent numerical instability and damping of the actuation values.)

The entire procedure outlined in the previous section is then repeated to derive the *feedback* gain matrix K_{ss}. It can be seen from Figures IV.9, IV.10, IV.11 and IV.12 that the matrix has non-zero values only at the desired locations of the controllers. Consequently, actuation is performed only at these sites. This is equivalent to controlling the problem with a finite number of actuators.

It can be seen from Figure IV.13 that flutter is controlled successfully even with a finite number of actuators. This is an important result, as it implies that this system can be implemented on a practical aerodynamic configuration.

B. 3-d Results

We now try to control the flutter of a realistic airplane wing. The wing is unswept and the cross-section is that of a 6 percent thick airfoil obtained by scaling down a NACA 0012 airfoil. The semi-span of the wing is 11.5 inches, and the chord is 4.56 inches. This corresponds to an aspect ratio of about 5.

Structurally, the wing is modeled as a plate of thickness 0.065 inches that is placed along the centerline of the wing-section. The density of the material of the wing is 0.003468 slug/sq. inch. The Young's modulus is 9.848×10^6 slug/sq. inch and the torsional rigidity is 3.639×10^6 slug/sq. inch.

The wing was operated under a freestream Mach number of 0.79 and a freestream dynamic pressure of 5241 Pascal.

The aero-structural integration was performed as discussed in Section II. The structure is modeled using 50 plate elements. The aerodynamic simulation is done on a $96 \times 32 \times 48$ grid. It can be seen from Figure IV.14 that the uncontrolled system diverges fairly rapidly. In the time frame considered, the plunge diverges from a negligible amount to 10 percent chord very quickly.

Our task, now, is to design a controller using the techniques described in the previous sections. It has been shown that the flutter of a wing can be studied by studying the dynamics of a section three quarters of the distance from the wing center-line to the tip. We identify the structural properties of the section

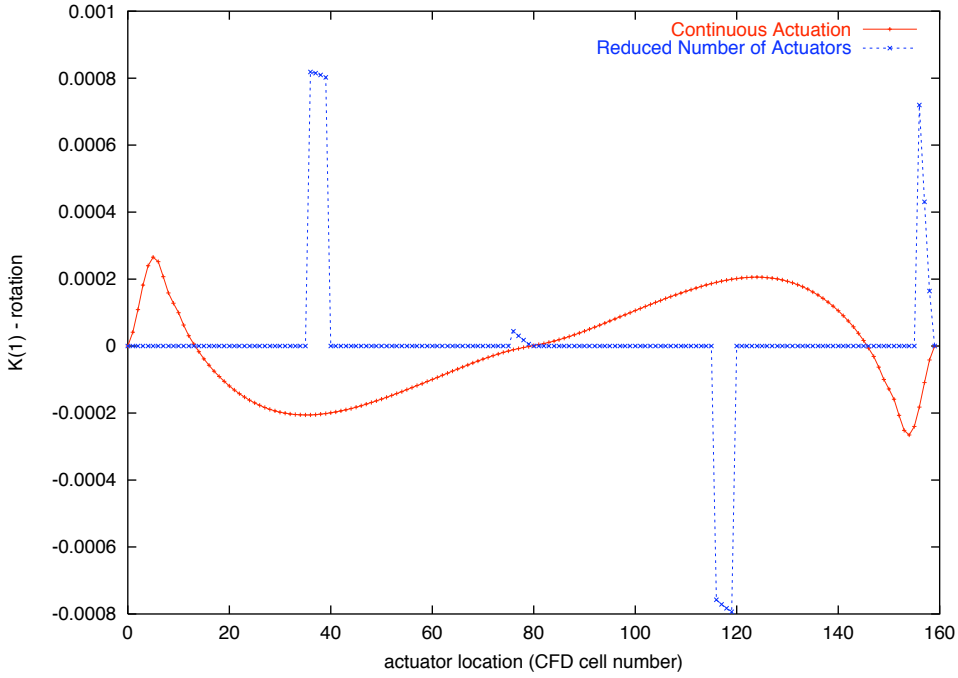

Figure IV.9. Coefficient of rotation angle vs. actuator number in the feedback gain matrix

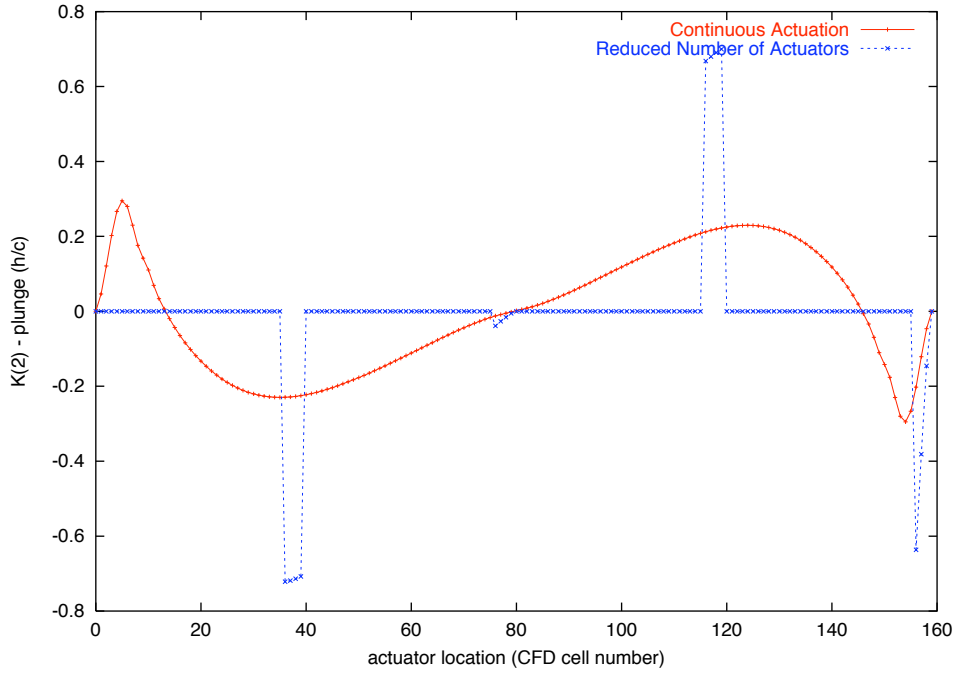

Figure IV.10. Coefficient of plunge vs. actuator number in the feedback gain matrix

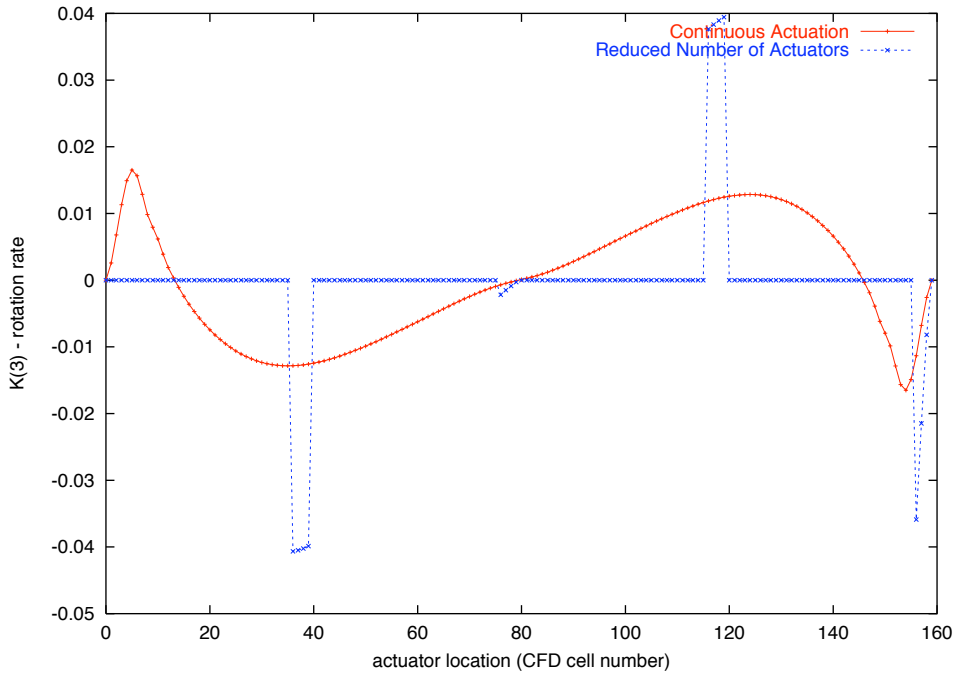

Figure IV.11. Coefficient of rotation angle rate vs. actuator number in the feedback gain matrix

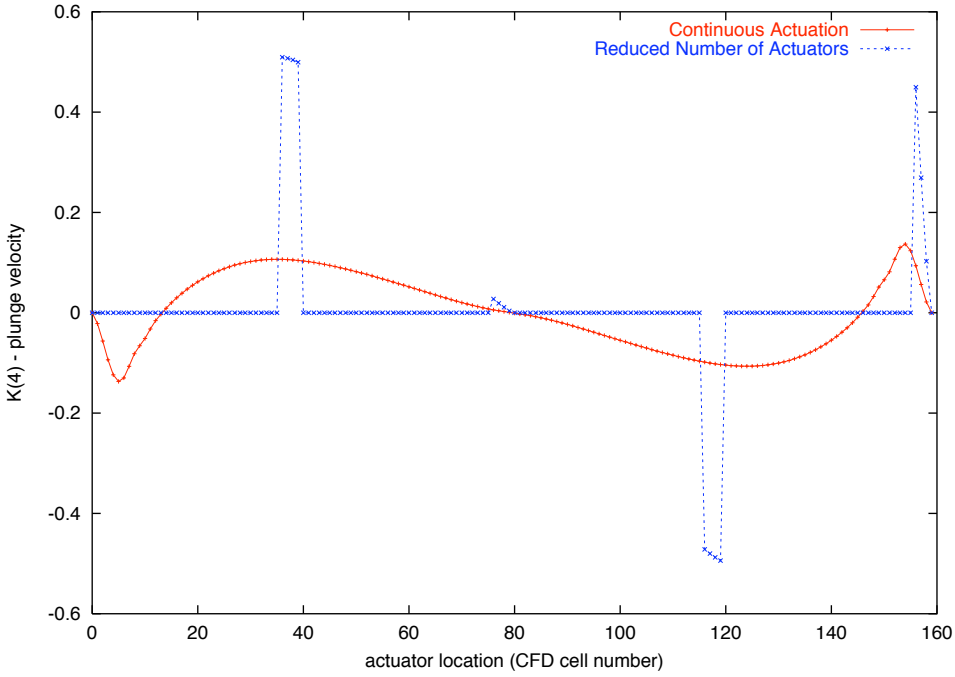

Figure IV.12. Coefficient of plunge velocity vs. actuator number in the feedback gain matrix

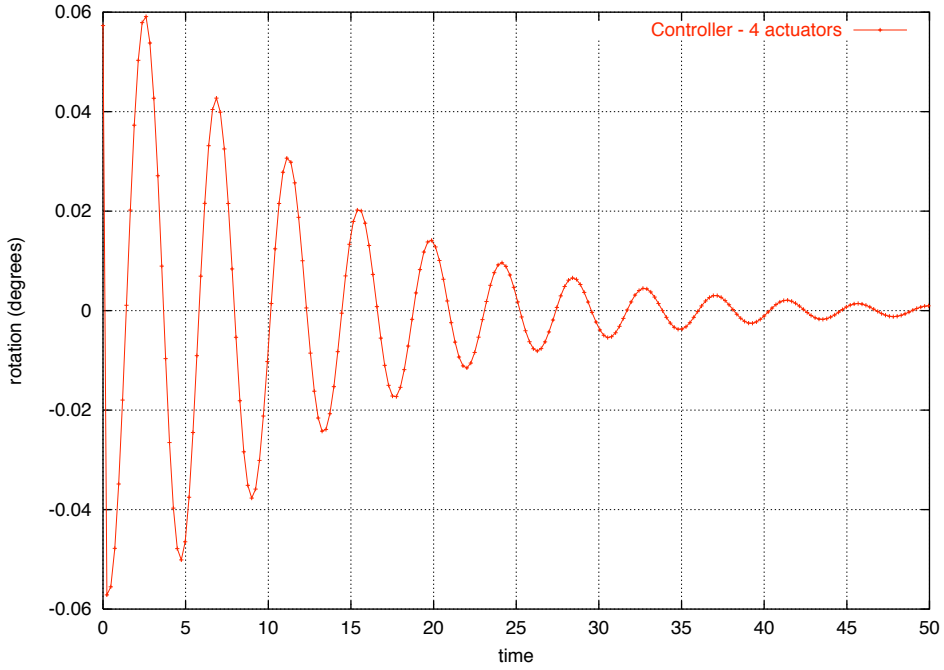

Figure IV.13. Variation of angle of attack (degrees) with time: with 4 actuators

located at this point, and model it using the typical section wing model, discussed previously. Following the techniques in the previous section, we quickly derive the *feedback* gain matrix K_{ss} for this section.

We make the assumption that this matrix is valid throughout the wing. This is a valid assumption, as the control is implemented in a *feedback* fashion. The tip is expected to go through the maximum deflection, and therefore will be subject to the maximum amount of control. (Since the control is proportional in nature). The root does not move at all, and thus there is no control applied at the root. The results of this simulation are shown in Figure IV.14. It can be seen that the control law thus derived is successful in controlling flutter. The mass fluxes at an actuator location at the tip, along the trailing edge are shown in Figure IV.15. Again, it can be seen that the mass fluxes required for control, when compared to the freestream mass flux of $\rho q_n = 1$ are very small.

Figures IV.16 and IV.17 show results from the complete 3-d simulation at identical times for the uncontrolled and controlled cases respectively. It can be seen, especially from the last pictures in both sequences that the deflections in the controlled case are smaller than those in the uncontrolled case. In fact, in the controlled case the wing settles into a limit cycle oscillation of small magnitude as can be seen from Figure IV.14. This is in spite of the fact that an approximate structural model was used in the calculation of the control law.

V. Conclusions and Future Work

In this work, we developed a *feedback* algorithm for the control of flutter. We demonstrated the effectiveness of this control law in 2-d and 3-d simulations. We also explored possibilities for the reduction in the number of actuators.

All the simulations in this work were done using an inviscid model. The next obvious step is to implement the control laws derived in this work in a fully viscous simulation. This will allow us to test the validity of our current simulations. It will also allow us to study the class of control problems where viscosity plays an important role: separation, transition, buffeting, etc.

Finally, in order for a *feedback* control system to be practical, it should be capable of generating control input in real time. To do this, it becomes necessary to work with reduced order models. The reduced order models used in this work were based on a set of parameters that were considered adequate to model the flow based on physical intuition. While this works well in practice, no guarantee can be made for a sophisticated

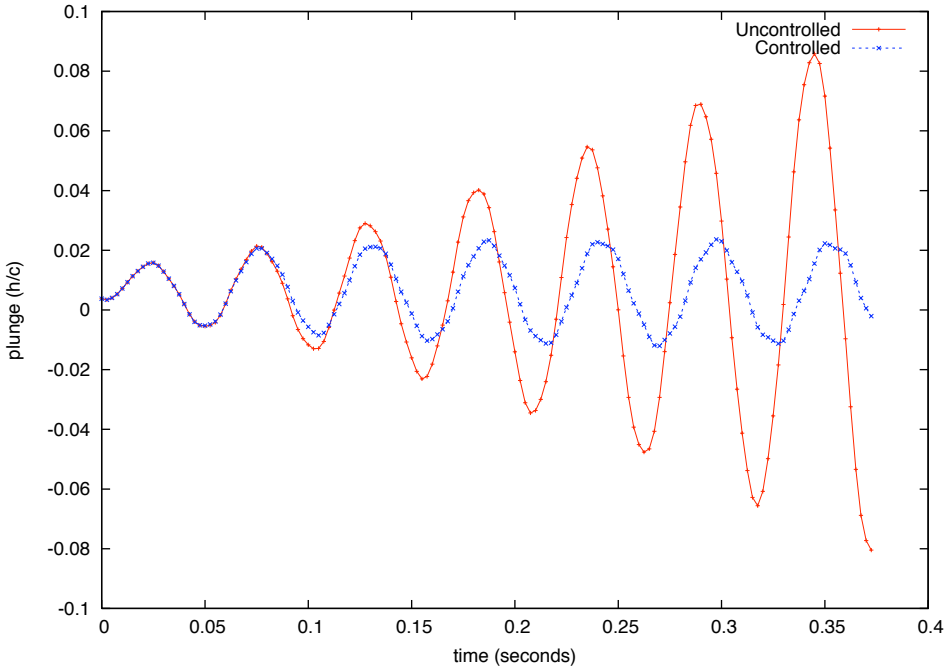

Figure IV.14. Variation of plunge h/c with time: controlled and uncontrolled cases

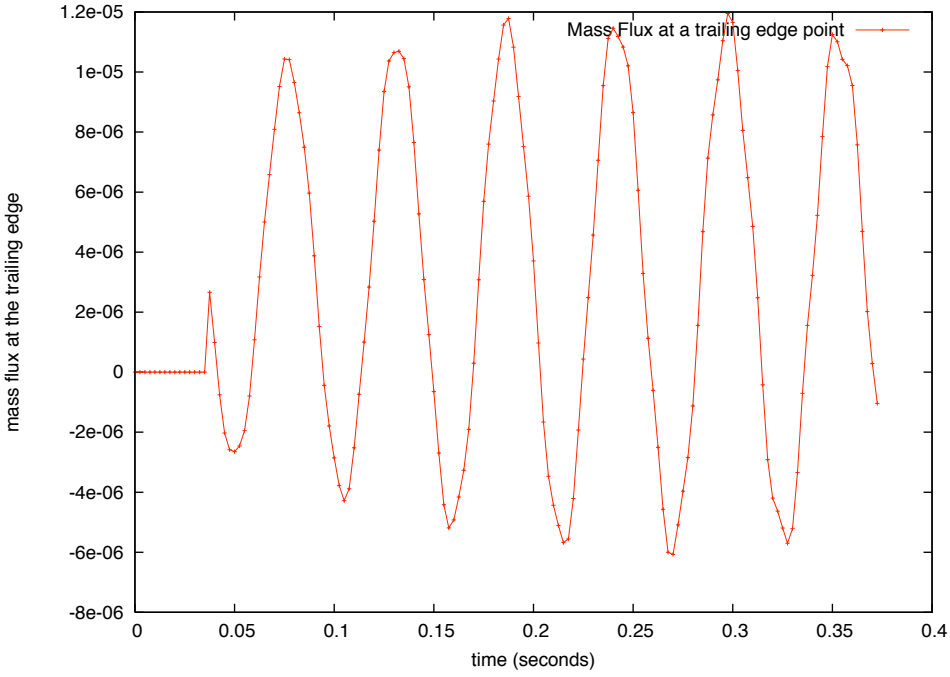

Figure IV.15. Blowing/Suction mass fluxes at a trailing edge point

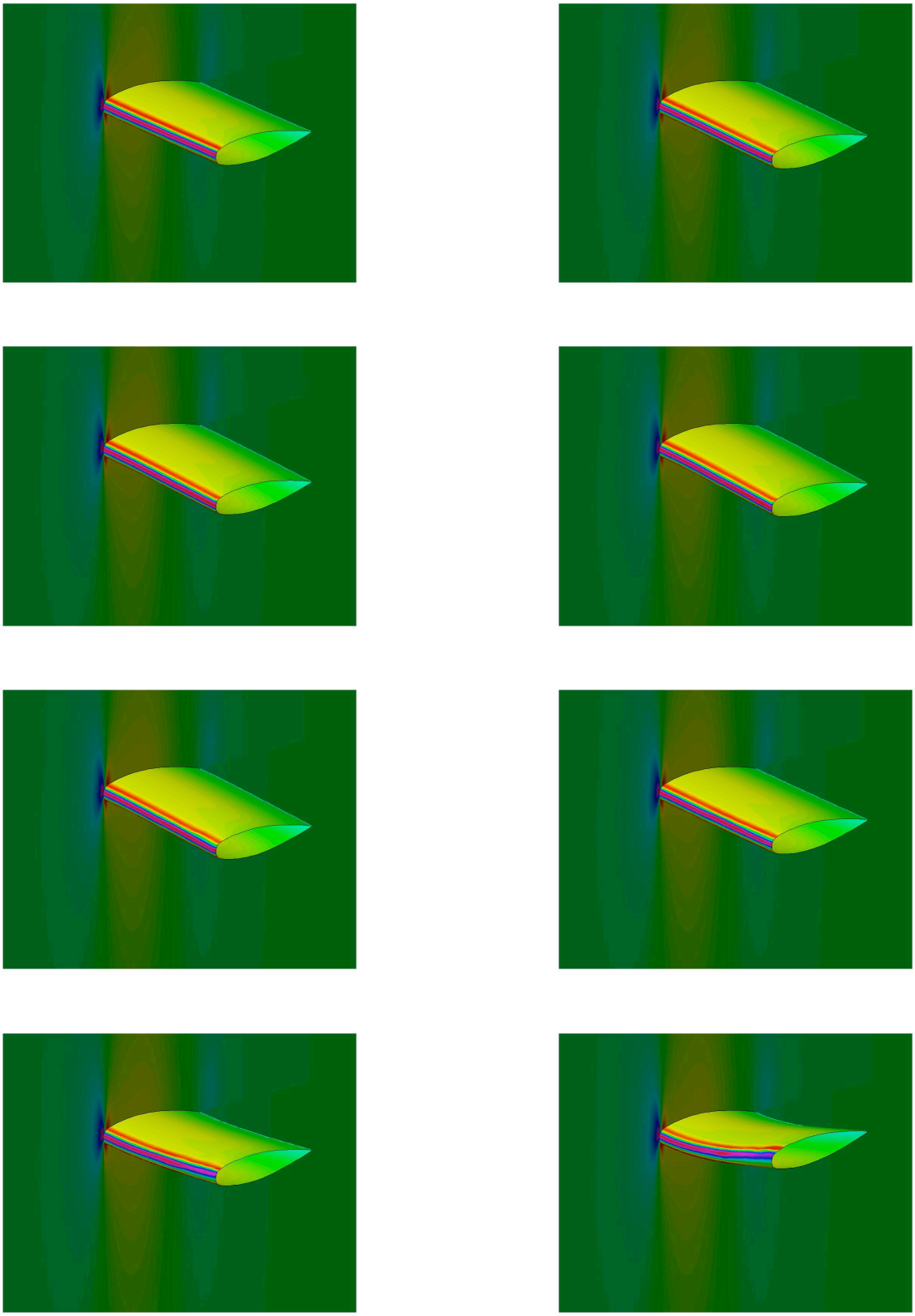

Figure IV.16. Uncontrolled simulation (Plunge variation at the tip shown in Figure IV.14)

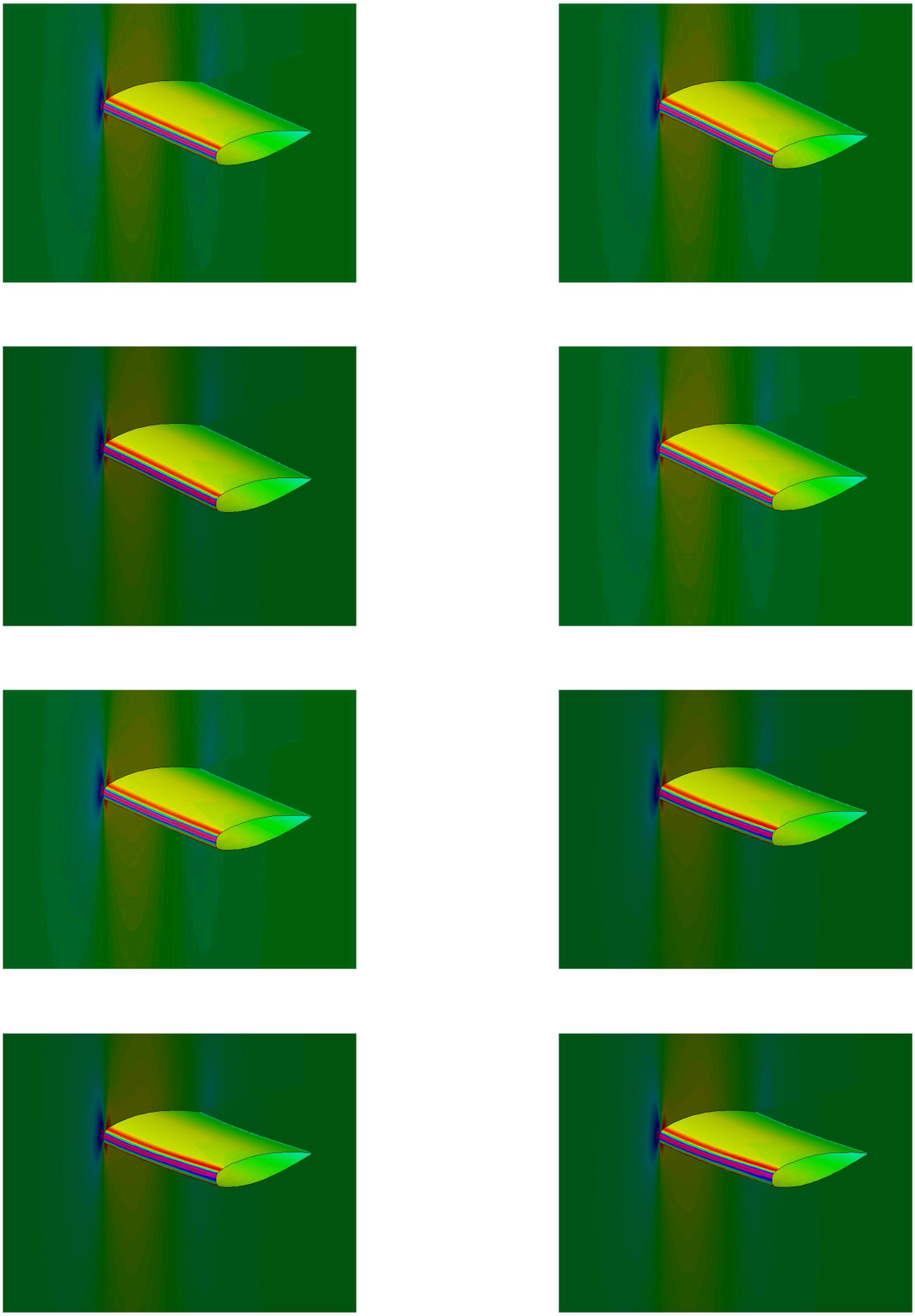

Figure IV.17. Controlled simulation (Plunge variation at the tip shown in Figure IV.14)

nonlinear system. For such cases we need algorithmic procedures to derive reduced order models from the complete nonlinear system. The control design procedure developed in this work needs to be modified to accommodate these reduced order models.

References

[1]Raymond L. Bisplinghoff, Holt Ashley, and Robert L. Halfman. *Aeroelasticity*. Dover Publications, 1996.

[2]Avi Seifert, Vassilis Theofilis, and Ronald D. Joslin. Issues in active flow control: Theory, simulation and experiment. AIAA Paper 2002-3277, 1st AIAA Flow Control Conference, Missouri, 2002.

[3]A. Glezer and M. Amitay. *Annual Review of Fluid Mechanics*, chapter Synthetic Jets. 2002.

[4]M. Amitay, M. Horvath, M. Michaux, and A. Glezer. Virtual aerodynamic shape modification at low angles of attack using synthetic jet actuators. AIAA Paper 2001-2975, 31st AIAA Fluid Dynamics Conference and Exhibit , Anaheim, CA, 2001.

[5]Ashley Tuck and Julio Soria. Active Flow Control of a NACA 0015 Airfoil using a ZNMF Jet. 15th AIAA Australian Fluid Mechanics Conference, December 2004.

[6]Hiroyuki Abe, Takehiko Segawa, Yoshihiro Kikushima, Hiro Yoshida, Akira Nishizawa, and Shohei Takagi. Towards smart control of separation around a wing, part 2. Technical report, Japan Aerospace Exploration Agency, 2003.

[7]Akira Nishizawa, Shohei Takagi, Hiroyuki Abe, Takehiko Segawa, and Hiro Yoshida. Towards smart control of separation around a wing, part 1. Technical report, Japan Aerospace Exploration Agency, 2003.

[8]Catalin Nae. Unsteady Flow Control using Synthetic Jet Actuators. AIAA Paper 2000-2403, Fluids 2000 Conference and Exhibit, Denver, Colarado, June 19-22, 2000.

[9]M. Samimy, M. Debiasi, E. Carabello, J. Malone, J. Little, H. Ozbay, M. O. Efe, P. Yan, X. Yuan, J. DeBonis, J. H. Myatt, and R. C. Camphouse. Exploring strategies for closed loop cavity flow control. AIAA Paper 2004-576 42nd AIAA Aerospace Sciences Meeting and Exhibit, Reno, Nevada, January 2004.

[10]G. V. Rajesh Kumar and Ashish Tewari. Active closed loop control of supersonic flow with transverse injection. AIAA Paper 2004-2699 2nd AIAA Flow Control Conference, Portland, Oregon, June 2004.

[11]Kelly Cohen, Stefan Siegel, and Thomas McLaughlin. Control issues in reduced order feedback flow control. AIAA Paper 2004-575, 42nd AIAA Aerospace Sciences Meeting and Exhibit, Reno, Nevada, January 2004.

[12]Antony Jameson. Aerodynamic Design via Control Theory. *Journal of Scientific Computing*, pages 233–260, 1988.

[13]Siva Nadarajah. *The Discrete Adjoint Approach to Aerodynamic Shape Optimization*. PhD thesis, Stanford University, 2003.

[14]T Theodorsen and I. E. Garrick. Mechanism of flutter, a theoretical and experimental investigation of the flutter problem. Technical report, N.A.C.A. Report 685, 1940.

[15]O. C. Zienkiewicz and R. L. Taylor. *The Finite Element Method*, volume 1. Butterworth-Heinemann, 2000.

[16]S. A. Brown. Displacement extrapolation for CFD + CSM aeroelastic analysis. AIAA Paper 1997-1090, 38th AIAA/ASME/ASCE/AHS/ASC Structures, Structural Dynamics, and Materials Conference and Exhibit, Kissimmee, Florida, April 1997.

[17]Karthik Palaniappan. *Algorithms for Automatic Feedback Control of Aerodynamic Flows*. PhD thesis, Stanford University, 2007.

[18]A. E. Bryson and Ho Yu-Chi. *Applied Optimal Control: Optimization, Estimation and Control*. Taylor and Francis In., 1988.